change, and related complications are often found in these ternary systems under arc-melting conditions, as might be expected.

**Acknowledgment.** Slavi C. Sevov provided valuable SEM information regarding compositions of $Zr_5Sn_{3+x}$ and $Zr_4Sn$ as well as data on the character of the segregation present in as-case samples of the former.

**Registry No.** Zr, 7440-67-7; Sn, 7440-31-5; $Sn_3Zr_5$, 58799-99-8; $Sn_4Zr_5$, 12211-14-2.

**Supplementary Material Available:** Listing of observed and calculated structure factor data for $Zr_5Sn_{3.18}$ (1 page). Ordering information is given on any current masthead page.

# Organometallic Acceptors in Molecular-Based Materials: Field-Dependent Magnetic Behavior of an Organovanadium Charge-Transfer Salt

David B. Morse

*School of Chemical Sciences and the Materials Research Laboratory, University of Illinois, Urbana, Illinois 61801*

*Received June 6, 1989*

The reaction of 2 equiv of tetramethyltetrathiofulvalene (TmTTF) with the organometallic acceptor (methylcyclopentadienyl)vanadium trichloride, $(MeCp)VCl_3$, followed by partial oxidation affords $[TmTTF]_3[\{(MeCp)VCl_2\}_2(\mu\text{-}O)]_2$ (1). The full structural parameters are reported with special emphasis on the mixed valence nature of both the cation $\{[TmTTF]_3^{2+}\}$ and anion $\{[\{(MeCp)VCl_2\}_2O]^-\}$ subunits, as well as the relationship of the two stacks within the lattice. Oriented single-crystal magnetic susceptibility data indicate that 1 develops weak ferromagnetic interactions along two dimensions ($XY$) at small applied fields (50 G). This behavior is dominant between 50 and 3 K. Crushed single-crystal samples require a higher applied field to induce the cooperative interactions. These cooperative interactions are suppressed at high applied fields. The zero-field ground state of 1 at 1.8 K is antiferromagnetic.

## Introduction

The development of novel materials based on molecular precursors is intimately tied to the harnessing of nature's "weak forces". Secondary interactions such as those between molecules can accumulate over large distances and develop into behavior unknown at the molecular level. This kind of "supramolecule" is a species quite distinct from its molecular parents since the long-range forces allow the physical behavior of a supramolecular material to be included in an external circuit. Many current areas of interest in chemistry center about systems that rely on the accumulation of these secondary forces for their device-oriented effects. This kind of device preparation is utilized (for example) in the assembly of microelectronics,[1] molecular recognition in biosensors,[2] and the complex behavior of liquid-crystal polymers.[3]

One area in which studies of molecular-based materials has focused is the field of charge-transfer salts. These materials are composed of individually charged molecules in a solid-state lattice that governs the interactions of the subunits. Many such salts exist,[4] and the control of their secondary forces through packing arrangements is often as important as the synthesis of the individual molecules.[5] The proper combination of acceptors and donors can result in supramolecular effects such as bulk ferromagnetism[6] or superconductivity.[7]

A distinct subclass of charge-transfer salts concerns the use of high oxidation state organometallic compounds as *acceptors*. The use of organometallic *donors* in the field has shown that structurally isolated molecules can develop cooperative magnetic phenomena,[8] but the area of organometallic acceptors has only recently been investigated. The preparation of novel solid-state materials based upon organometallic complexes could prove to be a rich area, considering the synthetic diversity in organometallic chemistry. To illustrate the potential of organometallic acceptors in molecular-based materials, this paper describes the first organometallic acceptor charge-transfer salt displaying ferromagnetic coupling.[9]

## Experimental Section

**Synthesis.** All reactions and characterizations were performed under a $N_2$ atmosphere using standard Schlenk line techniques and a Vacuum Atmospheres Dri-Lab. Solvents were distilled under nitrogen from appropriate drying agents ($CH_2Cl_2$, $P_4O_{10}$; toluene, Na; and hexanes, Na/K). The compound TmTTF was

(1) (a) Chao, S.; Wrighton, M. S. *J. Am. Chem. Soc.* **1987**, *109*, 2197. (b) Clarkson, M. A. *Byte* **1989**, *14*(5), 268.

(2) (a) Nagy, G.; Pungor, E. *J. Electroanal. Chem.* **1988**, *254*(20), 1. (b) Rechnitz, G. A. *Chem. Eng. News* **1988**, *66*(36), 24.

(3) Moore, J. S.; Stupp, S. I. *Macromolecules* **1988**, *21*, 1217.

(4) *Extended Linear Chain Compounds*; Miller, J. S., Ed.; Plenum: New York, 1982.

(5) Ferraro, J. R.; Williams, J. M. *Introduction to Synthetic Electrical Conductors*; Academic: Orlando, FL, 1987.

(6) Such as in $[(Me_5C_5)_2Fe][TCNE]$ (TCNE = tetracyanoethylene): (a) Miller, J. S.; Calabrese, J. C.; Epstein, A. J.; Bigelow, R. W.; Zhang, J. H.; Reiff, W. M. *J. Chem. Soc., Chem. Commun.* **1986**, 1026. (b) Miller, J. S.; Calabrese, J. C.; Rommelmann, H.; Chittipeddi, S. R.; Zhang, J. H.; Reiff, W. M.; Epstein, A. J. *J. Am. Chem. Soc.* **1987**, *109*, 769.

(7) Such as in derivatized tetrathiofulvalene complexes: Carlson, K. D.; Geiser, U.; Kini, A. M.; Wang, H. H.; Montgomery, L. K.; Kwok, W. K.; Beno, M. A.; Williams, J. M.; Cariss, C. S.; Crabtree, G. W.; Whangbo, M.-H.; Evain, M. *Inorg. Chem.* **1988**, *27*, 965, and references therein.

(8) Miller, J. S.; Epstein, A. J.; Reiff, W. M. *Chem. Rev.* **1988**, *88*, 201.

(9) Morse, D. B.; Rauchfuss, T. B.; Hendrickson, D. N. Presented in part at the 197th National Meeting of the American Chemical Society, Dallas, TX, Apr 1989; INORG 218.

0897-4756/90/2802-0033$02.50/0 

synthesized according to published procedure,[10] with an important modification in the purification of the intermediate "thione". The crude Decalin reaction solution was twice passed through a silica column, eluting with hexanes. The Decalin is eluted first and is discarded. The more slowly moving yellow thione may be eluted with $CH_2Cl_2$ and then crystallized from hexanes at low temperature. This procedure avoids the large-scale use of $Hg_2Cl_2$ and subsequent purification of the thione from HgS. The thione is somewhat air sensitive; solid samples will degrade over a period of months. The synthesis of $(MeCp)VCl_3$ has been described elsewhere.[16]

**[TmTTF][(MeCp)$VCl_3$].** A solution of $(MeCp)VCl_3$ (120 mg, 0.5 mmol) in 10 mL of $CH_2Cl_2$ was added to TmTTF (130 mg, 0.5 mmol) in 15 mL of $CH_2Cl_2$. The resulting reaction solution was evaporated to dryness, and the residue rinsed twice with 5 mL of toluene. The solid was extracted with 35 mL of $CH_2Cl_2$, and the filtrate slowly evaporated. The dark-purple microcrystalline solid was dried in vacuo for an 80% (200 mg) yield. Anal. Calcd for $C_{16}H_{19}S_4VCl_3$: C, 38.68; H, 3.85; V, 10.25. Found: C, 39.18; H, 3.97; V, 10.32. IR (KBr) 944, 860, 811 $cm^{-1}$.

**Reaction of 2 equiv of TmTTF with (MeCp)$VCl_3$.** A solution of $(MeCp)VCl_3$ (200 mg, 0.85 mmol) in 20 mL of $CH_2Cl_2$ was added to TmTTF (435 mg, 1.7 mmol) in 60 mL of $CH_2Cl_2$. The solution was allowed to stir for 1 h, then the solvent removed in vacuo. The resulting solid was extracted with 30 mL of $CH_2Cl_2$, and the filtrate reduced to dryness. The solid was washed with 10 mL of hexanes and dried in vacuo. The yield was 365 mg. Anal. Calcd for $C_{26}H_{31}S_8VCl_3$: C, 41.24; H, 4.13; V, 6.73. Found: C, 42.50; H, 4.27; V, 6.22. IR (KI) 928, 809 $cm^{-1}$.

**[TmTTF]$_3$[{(MeCp)$VCl_2$}$_2$O]$_2$ (1).** A solution of $(MeCp)VCl_3$ (205 mg, 0.9 mmol) in 20 mL of $CH_2Cl_2$ was added to TmTTF (440 mg, 1.7 mmol) in 40 mL of $CH_2Cl_2$. This solution was allowed to stir under $N_2$ for 3 days, by which time a fine dark-red precipitate was present (analyzing as [TmTTF][Cl]). The solution was filtered, and the filtrate reduced to ca. one-half the volume. The product was crystallized from this solution at −25 °C. The regular rectangular blocks were isolated for a 20% (70 mg) yield. Anal. Calcd for $C_{27}H_{32}S_6V_2Cl_4O$: C, 40.11; H, 3.99; V, 12.60. Found: C, 40.33; H, 4.14; V, 12.48. IR (KBr) 806, 823, 875, 927 $cm^{-1}$.

**Physical Measurements.** Microanalyses were performed by the University of Illinois Microanalytical Laboratory, and FT-IR measurements on pressed pellets were carried out on a Perkin-Elmer Model 1750 Fourier transform spectrophotometer linked to a Perkin-Elmer 7700 data station. Variable-temperature magnetic susceptibility experiments were performed on a S.H.E. Ind. VTS-50 Series 800 SQUID susceptometer; a value of $-456.41 \times 10^{-6}$ cgsu for the mole unit [TmTTF]$_{1.5}$[{(MeCp)$VCl_2$}$_2$O] was used for diamagnetic correction. X-ray analysis was performed by the School of Chemical Sciences Crystallography Center.

**Crystallography.** The structure of [TmTTF]$_3$[{(MeCp)$VCl_2$}$_2$O]$_2$ was determined from a crystal obtained from a typical synthesis of the salt. The green, opaque crystal selected (0.2 × 0.5 × 0.6 mm) was mounted under an inert atmosphere by using a trace amount of grease inside a 0.7-mm thin-walled, tapered glass capillary. Data collection was performed at 26 °C on a Syntex $P2_1$ automated four-circle diffractometer with graphite crystal monochromated molybdenum radiation ($\lambda(K\bar{\alpha})$ = 0.71073 Å).

A unique set of 15 reflections was carefully selected and centered to determine cell parameters (triclinic $P\bar{1}$; $a$ = 12.984 (5), $b$ = 13.154 (4), $c$ = 10.770 (4) Å; $\alpha$ = 98.45 (3), $\beta$ = 93.56 (3), $\gamma$ = 70.22 (3)°; $V$ = 1712 (1) Å$^3$; $Z$ = 2; $\rho_{calc}$ = 1.568). From 6661 measured intensities, 6058 were processed, resulting in 4034 observed reflections with $I > 2.58\sigma(I)$. Total crystal exposure time was 64.25 h. The data were corrected for Lorentzian, anomalous dispersion, and polarization effects and numerically corrected for absorption. Diffraction intensity was observed to the upper $2\theta$ limit (50°).

The structure was solved by direct methods (MULTAN); correct positions for two vanadium, four chlorine, and two sulfur atoms were deduced from an $E$ map. A weighted difference Fourier gave positions for all but three of the remaining non-hydrogen atoms. Subsequent least squares-difference Fourier calculations located

**Table I. Positional Parameters for [TmTTF]$_3$[{(MeCp)$VCl_2$}$_2$O]$_2$**

| | $x/a$ | $y/b$ | $z/c$ |
|---|---|---|---|
| V1 | 0.77727 (8) | 0.36515 (7) | 0.03356 (9) |
| V2 | 0.75473 (8) | 0.36666 (8) | −0.29779 (9) |
| Cl1 | 0.9160 (1) | 0.2089 (1) | 0.0665 (2) |
| Cl2 | 0.6251 (1) | 0.3166 (1) | 0.0524 (2) |
| Cl3 | 0.8549 (1) | 0.1995 (1) | −0.3968 (2) |
| Cl4 | 0.8722 (2) | 0.4619 (2) | −0.3162 (2) |
| S31 | 0.3399 (1) | −0.0210 (1) | 0.4668 (1) |
| S34 | 0.4037 (1) | 0.1732 (1) | 0.5272 (2) |
| S41 | 0.3149 (1) | −0.0535 (1) | 0.7952 (2) |
| S44 | 0.3119 (1) | 0.1705 (1) | 0.8385 (1) |
| S47 | 0.5757 (1) | 0.0861 (1) | 0.8624 (1) |
| S50 | 0.5802 (1) | 0.1387 (1) | 0.8215 (1) |
| S50 | 0.5802 (1) | 0.1387 (1) | 0.8215 (1) |
| O | 0.7811 (3) | 0.3462 (3) | −0.1384 (3) |
| C11 | 0.8331 (5) | 0.4592 (5) | 0.2135 (6) |
| C12 | 0.7200 (5) | 0.5033 (5) | 0.1993 (6) |
| C13 | 0.6952 (7) | 0.5469 (5) | 0.0890 (7) |
| C14 | 0.7960 (8) | 0.5303 (5) | 0.0292 (7) |
| C15 | 0.8803 (6) | 0.4738 (5) | 0.1054 (7) |
| C16 | 0.8959 (6) | 0.4038 (6) | 0.3218 (7) |
| C21 | 0.6200 (5) | 0.3753 (6) | −0.4558 (6) |
| C22 | 0.6306 (6) | 0.4746 (6) | −0.4306 (8) |
| C23 | 0.6022 (6) | 0.5174 (7) | −0.3039 (8) |
| C24 | 0.5736 (5) | 0.4424 (7) | −0.2517 (7) |
| C25 | 0.5856 (5) | 0.3499 (7) | −0.3406 (8) |
| C26 | 0.6378 (7) | 0.3037 (7) | −0.5765 (8) |
| C32 | 0.2346 (5) | 0.1061 (5) | 0.4782 (5) |
| C33 | 0.2637 (5) | 0.1938 (5) | 0.5066 (5) |
| C35 | 0.4459 (4) | 0.0317 (4) | 0.4998 (5) |
| C36 | 0.1196 (5) | 0.1026 (5) | 0.4544 (7) |
| C37 | 0.1896 (6) | 0.3106 (5) | 0.5269 (6) |
| C42 | 0.1863 (5) | 0.0479 (5) | 0.7942 (5) |
| C43 | 0.1848 (5) | 0.1511 (5) | 0.8143 (5) |
| C45 | 0.3889 (5) | 0.0337 (4) | 0.8235 (5) |
| C46 | 0.5027 (5) | −0.0020 (4) | 0.8346 (5) |
| C48 | 0.7058 (4) | −0.0160 (4) | 0.8605 (5) |
| C49 | 0.7066 (4) | −0.1178 (4) | 0.8408 (5) |
| C51 | 0.0907 (5) | 0.0094 (5) | 0.7696 (7) |
| C52 | 0.0854 (5) | 0.2523 (5) | 0.8190 (6) |
| C53 | 0.7998 (5) | 0.0270 (5) | 0.8802 (6) |
| C54 | 0.8063 (5) | −0.2198 (5) | 0.8370 (6) |
| H12 | 0.6674 | 0.5029 | 0.2580 |
| H13 | 0.6230 | 0.5823 | 0.0576 |
| H14 | 0.8040 | 0.5538 | −0.0488 |
| H15 | 0.9571 | 0.4490 | 0.0877 |
| H16a | 0.9730 | 0.3815 | 0.3069 |
| H16b | 0.8759 | 0.3411 | 0.3291 |
| H16c | 0.8786 | 0.4537 | 0.3981 |
| H22 | 0.6537 | 0.5109 | −0.4890 |
| H23 | 0.6031 | 0.5868 | −0.2623 |
| H24 | 0.5490 | 0.4514 | −0.1673 |
| H25 | 0.5739 | 0.2838 | −0.3285 |
| H26a | 0.6244 | 0.2377 | −0.5675 |
| H26b | 0.7120 | 0.2863 | −0.6021 |
| H26c | 0.5887 | 0.3402 | −0.6387 |
| H36a | 0.1221 | 0.0282 | 0.4355 |
| H36b | 0.0873 | 0.1410 | 0.3848 |
| H36c | 0.0765 | 0.1365 | 0.5279 |
| H37a | 0.2331 | 0.3572 | 0.5466 |
| H37b | 0.1412 | 0.3210 | 0.5950 |
| H37c | 0.1474 | 0.3282 | 0.4518 |
| H51a | 0.1153 | −0.0689 | 0.7586 |
| H51a | 0.1153 | −0.0689 | 0.7586 |
| H51b | 0.0528 | 0.0352 | 0.6949 |
| H51c | 0.0420 | 0.0371 | 0.8395 |
| H52a | 0.1077 | 0.3156 | 0.8348 |
| H52b | 0.0386 | 0.2533 | 0.8851 |
| H52c | 0.0465 | 0.2523 | 0.7402 |
| H53a | 0.7720 | 0.1052 | 0.8919 |
| H53b | 0.8463 | 0.0016 | 0.8082 |
| H53c | 0.8412 | 0.0018 | 0.9533 |
| H54a | 0.7837 | −0.2830 | 0.8212 |
| H54b | 0.8447 | −0.2198 | 0.9161 |
| H54c | 0.8537 | −0.2213 | 0.7713 |

(10) Ferraris, J. P.; Poehler, T. O.; Bloch, A. N.; Cowan, D. O. *Tetrahedron Lett.* **1973**, *27*, 2553.

the remaining atoms. Hydrogen atoms were fixed in "idealized" positions. A listing of positional parameters is provided in Table I. Non-hydrogen atoms were refined with anisotropic thermal coefficients, and a group isotropic thermal parameter was varied for the hydrogen atoms. The highest peak in the final difference Fourier map ($+0.75 > e/Å^3 > -0.42$) indicated a minor disorder in the position of one methyl group between C21 and C23. A final analysis of variance between observed and calculated structure factors showed a slight dependence on sin $\theta$; $R = 0.050$, $R_w = 0.059$.

## Results

**Synthesis.** The reaction between $(MeCp)VCl_3$ (MeCp = $\eta^5$-$MeC_5H_4$) and TmTTF (tetramethyltetrathiofulvalene) can result in the formation of two materials with differing TmTTF:$(MeCp)VCl_3$ ratios. When $(MeCp)VCl_3$ is added to 1 equiv of TmTTF, the previously characterized 1:1 charge-transfer salt[11] immediately precipitates from solution. This poorly soluble material (ca. 0.5 mg/mL) is identified by diagnostic[12] infrared absorptions at 811, 860, and 944 $cm^{-1}$. When $(MeCp)VCl_3$ is added to 2 equiv of TmTTF, no precipitation occurs. Even upon concentration of the solution, no 1:1 adduct precipitates. According to the infrared spectrum of the highly soluble (ca. 20 mg/mL) isolated solid (809 and 928 $cm^{-1}$), it is not the 1:1 salt, nor is it the oxidized oxo-bridged product (vide infra), nor is it a superposition of the two. There is however an indication of neutral TmTTF in the IR (438 $cm^{-1}$) as well as in the microanalysis data. The latter suggest an approximate composition of $[TmTTF]_{2.3}[(MeCp)VCl_3]$.[13]

Initial attempts to crystallize the highly air sensitive 2:1 phase led to the isolation of $[TmTTF]_3[\{(MeCp)VCl_2\}_2O]_2$ (1). Solutions of $[TmTTF]_2[(MeCp)VCl_3]$ when slowly exposed to $O_2$ and cooled afford large rectangular crystals of sparingly soluble (ca. 0.1 mg/mL) 1 in 20% yield. Under these conditions, the thin platelike crystals of $[TmTTF][(MeCp)VCl_3]$ do not form. The well-formed single crystals of 1 may be isolated from minor amounts of bright orange TmTTF by careful washing with toluene or removal by hand. Purity can be assayed by microanalysis and by diagnostic infrared absorptions at 806, 823, 875, and 927 $cm^{-1}$.

**Crystallography.** An X-ray analysis was performed at room temperature on a single crystal of 1 which diffracted in the triclinic space group $P\bar{1}$. The crystal and unit cell axes are oriented as in Figure 1,[14] while Figure 2 provides a stereoscopic packing diagram of the primary components. The asymmetric unit is comprised of 1.5 TmTTF molecules and an organometallic oxo-bridged dimer $\{(MeCp)VCl_2\}_2O$.

The TmTTF's stack in an A·A·B pattern with inversion-related A components and a B component with its own inversion center (Figure 3). This stack is along the *c* axis with every third (B) TmTTF tilted both 3° from the *c* axis and 3° from the *a* axis. While the $S_4C_2$ core of A exhibits somewhat contracted C–S bond lengths compared to B, and the interior C=C in the B component is somewhat shorter than in A, and the exterior C=C bonds of both A and B are equally short (Table II). Thus, no clear pattern of bond lengths or angles exists in the two different types of TmTTF to indicate the individual degree of oxidation. The interlamellar distances between the TmTTF units in 1 are typical at an average 3.56 (1) Å.

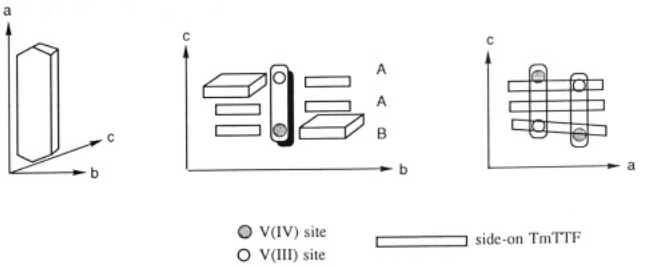


**Figure 1.** Illustration of crystal and molecular axes of $[TmTTF]_3[\{(MeCp)VCl_2\}_2O]_2$.

While the charge distribution is not clear within the organic stack, the charge on the organometallic subunit is well defined (Figure 4). The vanadium–oxygen bonds are asymmetric (1.833 (4) vs. 1.722 (4) Å, ∠VOV = 163.0 (2)°), indicating that at least partially localized $V^{III}$–$V^{IV}$ metal centers exist,[15] leading to an overall charge assignment for the subunit of −1 per VOV unit (Table III). Note that the $V^{III}$–$V^{IV}$ asymmetry is opposed for each pair of anions, and that *both the anion and cation are thus mixed valence*. The V–Cl distances (2.283 (2)–2.311 (2) Å) are longer than those of $(MeCp)VCl_3$[16] and somewhat shorter than those in $[TmTTF][(MeCp)VCl_3]$. The only van der Waals contacts are relatively long Cl···S (3.622 (2) Å), Cl···H (2.836 (6)–2.954 (7) Å), and S···H (3.077 (8)–3.116 (8) Å) distances. (The sum of van der Waals radii are 3.86, 2.96, and 3.24 Å, respectively.)

Several nonstoichiometric TTF salts are known, but none displays the combination of A·A·B pattern and highly delocalized charge structure of 1. For instance, $(TTF)_3(BF_4)_2$ consists of parallel TTF moieties with $(TTF^+)_2TTF^0$ packing.[17] One the other hand, $(TTF)_3(SnCl_6)$ contains equally spaced, nearly identical TTF moieties, indicating delocalized charges.[18] Other incompletely described salts are known.[19]

**Susceptibility.** Due to the small size of the crystals, single-crystal magnetization studies were not possible. However, susceptibility data were obtained by adhering three to four small single crystals together with grease.[20] The crystals were then aligned on the basis of their well-defined crystal morphology.

Oriented crystalline samples of 1 exhibit two magnetic responses depending upon applied field and temperature. For small fields, the crystals exhibit gradually decreasing $\chi T$ with decreasing temperature, indicating a thermal

(11) Morse, D. B.; Rauchfuss, T. B.; Wilson, S. R. *J. Am. Chem. Soc.* **1988**, *110*, 2646.

(12) The diagnostic IR bands for the complex could not be accurately assigned but are probably related to C–S stretches; while the IR bands for $TmTTF^{n+}$ are not reported, the general trends may be observed with TTF: Bozio, R.; Zanon, I.; Girlando, A.; Pecile, C. *J. Phys. Chem.* **1979**, *71*, 2282.

(13) Morse, D. B. Ph.D. Thesis, University of Illinois at Urbana–Champaign, 1989.

(14) Preliminary packing diagrams have been reported.[11]

(15) Several V(III)–V(III) μ-oxo dimers are known. (a) $[V(triazacyclononane)(acetate)]_2O$, V–O 1.79 Å: Köppen, M.; Fresen, G.; Wieghardt, K.; Llusar, R. M.; Nuber, B.; Weiss, J. *Inorg. Chem.* **1988**, *27*, 721. (b) $[V(SCH_2CH_2NMe_2)_2]_2O$, 1.80 and 1.82 Å: Money, J. K.; Folting, K.; Huffman, J. C.; Cristou, G. *Inorg. Chem.* **1987**, *26*, 944. (c) $[VCl_2(THF)_3]_2O$, 1.77 Å: Chandrasekhar, P.; Bird, P. H. *Inorg. Chem.* **1984**, *23*, 3677.

(16) Morse, D. B.; Hendrickson, D. N.; Rauchfuss, T. B.; Wilson, S. R. *Organometallics* **1988**, *7*, 496.

(17) Legros, J.-P.; Bousseau, M.; Valade, L.; Cassoux, P. *Mol. Cryst. Liq. Cryst.* **1983**, *100*, 181.

(18) Kondo, K.; Matsubayashi, G.; Tanaka, T.; Yoshioka, H.; Nakatsu, K. *J. Chem. Soc., Chem. Commun.* **1984**, 379.

(19) In general, other reported salts have not provided many details concerning the solid-state interactions of the material: (a) $(TmTTF)_3(DETCNQ)_2$: Fabre, J.-M.; Vigroux, M.; Torreilles, E.; Giral, L.; Chasseau, D. *Tetrahedron Lett.* **1980**, *21*, 607. (b) $(TTF)_7I_5$: Johnson, C. R.; Watson, C. R. *J. Chem. Phys.* **1976**, *64*, 2271. (c) $(BEDT\text{–}TTF)_3(ClO_4)_2$: Kobayashi, H.; Kato, R.; Mori, T.; Kobayashi, A.; Sasaki, Y.; Saito, G.; Enoki, T.; Inokuchi, H. *Mol. Cryst. Liq. Cryst.* **1984**, *107*, 33.

(20) With this procedure, no movement of the crystals was observed after any of the susceptibility experiments.

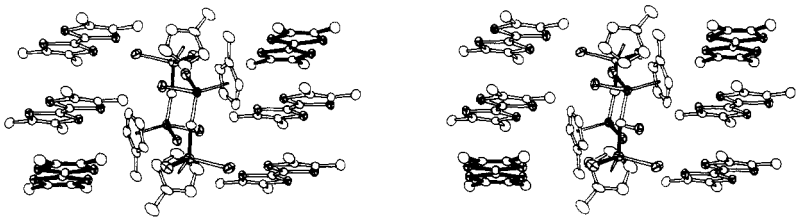

**Figure 2.** Stereoscopic packing diagram of $[TmTTF]_3[\{(MeCp)VCl_2\}_2O]_2$.

**Table II. Bond Distances (angstroms) and Angles (degrees) for the TmTTF Subunits of $[TmTTF]_3[\{(MeCp)VCl_2\}_2O]_2$**

| | | | |
|---|---|---|---|
| S31–C32 | 1.759 (6) | C32–C33 | 1.320 (8) |
| C33–S34 | 1.750 (6) | S31–C35 | 1.736 (5) |
| S34–C35 | 1.737 (5) | C35–C35[a] | 1.370 (7) |
| C32–C36 | 1.514 (8) | C33–C37 | 1.503 (8) |
| S41–C42 | 1.750 (6) | C42–C43 | 1.338 (8) |
| C43–S44 | 1.752 (6) | S41–C45 | 1.714 (5) |
| S44–C45 | 1.726 (5) | C45–C46 | 1.394 (8) |
| C46–S47 | 1.714 (5) | S47–C48 | 1.765 (6) |
| C48–C49 | 1.322 (8) | C46–S50 | 1.728 (5) |
| C49–S50 | 1.749 (5) | C42–C51 | 1.487 (9) |
| C43–C52 | 1.504 (8) | C48–C53 | 1.501 (8) |
| C49–C54 | 1.514 (8) | | |
| C32–S31–C35 | 95.7 (3) | S31–C32–C33 | 117.1 (4) |
| S31–C32–C36 | 115.9 (4) | C33–C32–C36 | 127.0 (5) |
| C32–C33–S34 | 117.1 (4) | C32–C33–C37 | 127.3 (5) |
| S34–C33–C37 | 115.6 (4) | C33–S34–C35 | 96.0 (3) |
| S31–C35–S34 | 114.2 (3) | S31–C35=C35[a] | 123.4 (4) |
| S34–C35=C35[a] | 122.3 (4) | C42–S41–C45 | 96.1 (3) |
| S41–C42–C43 | 116.6 (4) | S41–C42–C51 | 116.2 (4) |
| C43–C42–C51 | 127.2 (5) | C42–C43–S44 | 116.5 (4) |
| C42–C43–C52 | 126.8 (5) | S44–C43–C52 | 116.7 (4) |
| C43–S44–C45 | 95.8 (3) | S41–C45–S44 | 115.0 (3) |
| S41–C45–C46 | 123.1 (4) | S44–C45–C46 | 121.9 (4) |
| C45–C46–S47 | 122.6 (4) | C45–C46–S50 | 122.1 (4) |
| S47–C46–S50 | 115.2 (3) | C46–S47–C48 | 95.8 (3) |
| S47–C48–C49 | 116.1 (4) | S47–C48–C53 | 114.3 (4) |
| C49–C48–C53 | 129.6 (5) | C48–C49–S50 | 117.5 (4) |
| C48–C49–C54 | 126.7 (5) | S50–C49–C54 | 115.8 (4) |
| C46–S50–C49 | 95.4 (3) | | |

[a] Equivalent position $(1 - x, y, 1 - z)$.

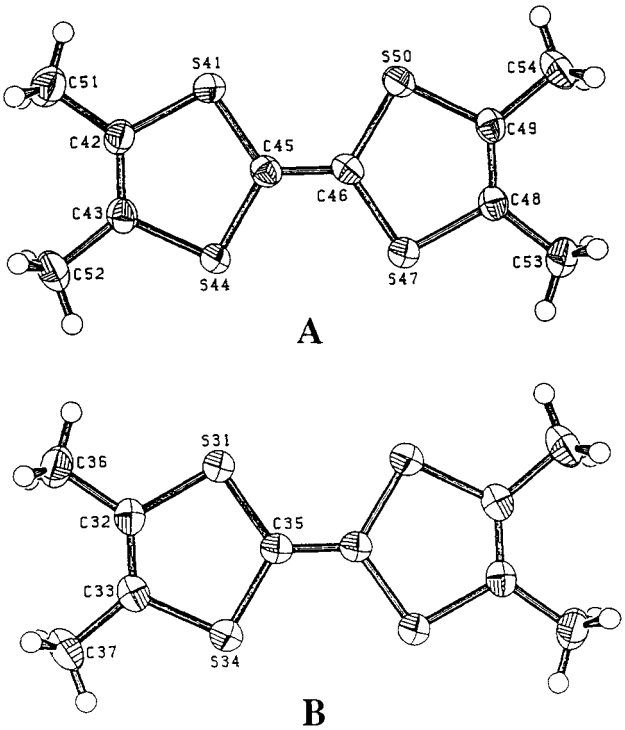


**Figure 3.** A- and B-type TmTTF subunits of $[TmTTF]_3[\{(MeCp)VCl_2\}_2O]_2$.

depopulation of a manifold of energy states (Figure 5). An increase in susceptibility begins between 50 and 20 K; the effect is most pronounced along the *b* axis and only somewhat less so along the *a* axis. The *c* (stacking) axis susceptibility displays only a slight increase in $\chi T$ below 50K. The response reaches a maximum at 3.5 K, whereupon $\chi T$ precipitously decreases. A spin-only consideration of the susceptibility at 3.5 K indicates that weak ferromagnetic coupling is being observed: the sum of $\chi T_{obs}$ for each axis (2.6 emu K) is *greater* than that expected for a summation of independent (spin-only) $TmTTF^+$ ($S = {}^1/_2$, $\chi T = 0.375$) and $\{(MeCp)VCl_2\}_2O^-$ ($S = {}^3/_2$, $\chi T = 1.876$) magnetic units ($\Sigma = 2.251$).[21]

As the applied field is raised, the susceptibilities along the ordering axes do not respond equally. By $H_{ap} = 1500$ G, the *c* axis exhibits no ferromagnetic coupling, and only a weak susceptibility enhancement is still present along the *a* axis (Figure 6). The *b* axis still displays weak coupling, although the susceptibility of this domain is now superimposed upon a much larger (high temperature) antiferromagnetic response.

Polycrystalline samples display susceptibility profiles that are qualitatively different than single-crystal samples (Figure 7). For low temperatures and fields, the solid

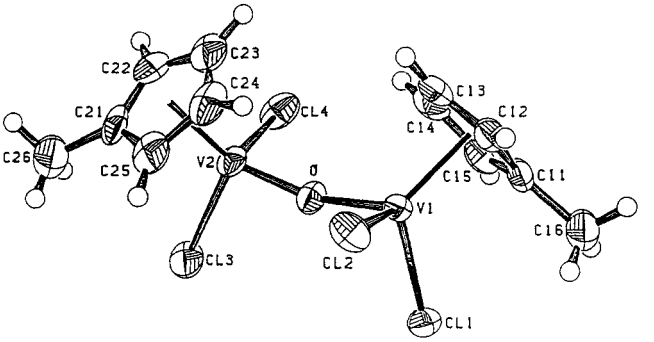


**Figure 4.** $\{(MeCp)VCl_2\}_2O$ subunit of $[TmTTF]_3[\{(MeCp)VCl_2\}_2O]_2$.

exhibits antiferromagnetic behavior, and then at moderate fields the weak ferromagnetic interactions. At even higher fields, antiferromagnetic behavior again sets in. (The high-temperature region is indicative of thermal depopulation of widely separated energy levels at both field levels, as in the low-field single-crystal profiles.) Magnetization studies on polycrystalline samples indicate effective field saturation only at 1.8 K and ca. 50 kG. Spontaneous zero-field magnetization was not observed.

Finally, it should be noted that single crystals of the complex eventually fracture along planes normal to the *c* axis when quickly cooled to 77 K or less. Samples

(21) Plots of $1/\chi$ are *not* linear in any region of the 300–2 K range. Between 50 and ca. 5 K, the slopes of *a* and *b* axis data intercept the temperature axis at decreasingly *positive* values.

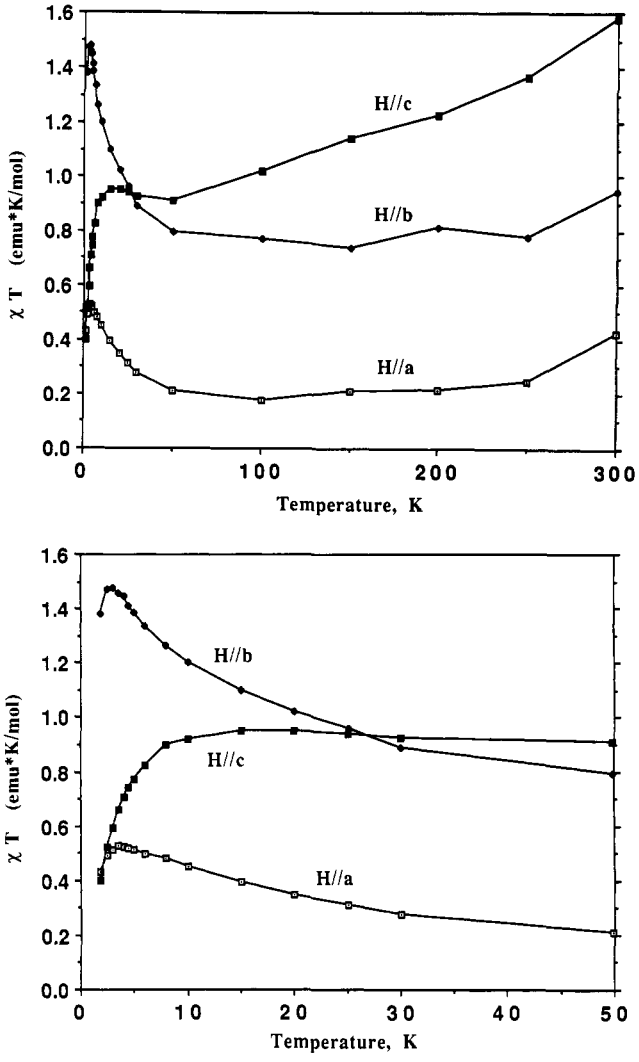


**Figure 5.** $\chi T$ versus temperature for $[TmTTF]_3[\{(MeCp)VCl_2\}_2O]_2$ at an applied field of 50 G (top, 300–1.8 K; bottom, expanded $T < 50$ K).

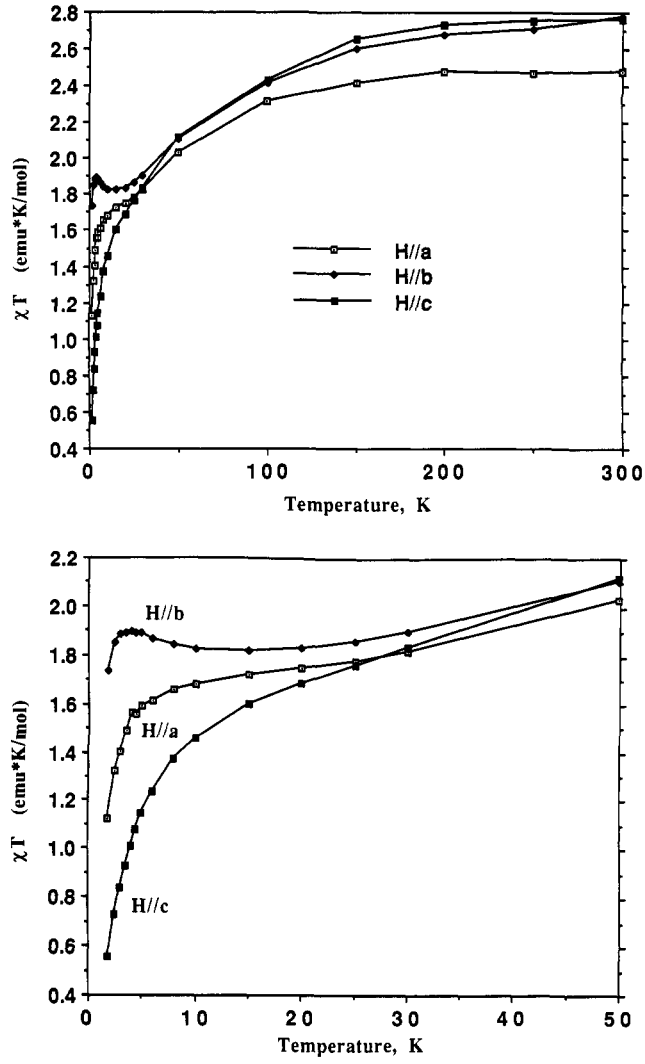


**Figure 6.** $\chi T$ versus temperature for $[TmTTF]_3[\{(MeCp)VCl_2\}_2O]_2$ at an applied field of 1500 G (top, 300–1.8 K; bottom, expanded $T < 50$ K).

**Table III. Bond Distances (angstroms) and Angles (degrees) for the $\{(MeCp)VCl_2\}_2O$ Subunits of $[TmTTF]_3[\{(MeCp)VCl_2\}_2O]_2$**

| | | | |
|---|---|---|---|
| V1–Cl1 | 2.286 (2) | V1–Cl2 | 2.301 (2) |
| V2–Cl3 | 2.283 (2) | V2–Cl4 | 2.311 (2) |
| V1–O | 1.833 (4) | V2–O | 1.772 (4) |
| V1–Cp1 | 1.968 (6) | V2–Cp2 | 1.976 (7) |
| Cl1–V1–Cl2 | 101.79 (7) | Cl1–V1–O | 98.0 (1) |
| Cl1–V1–Cp1 | 117.1 (2) | Cl2–V1–O | 97.5 (1) |
| Cl2–V1–Cp1 | 119.3 (2) | O–V1–Cp1 | 119.1 (2) |
| Cl3–V2–Cl4 | 99.79 (7) | Cl3–V2–O | 101.0 (1) |
| Cl3–V2–Cp2 | 117.5 (2) | Cl4–V2–O | 98.9 (1) |
| Cl4–V2–Cp2 | 116.5 (2) | O–V2–Cp2 | 119.6 (2) |
| V1–O–V2 | 163.0 (2) | | |

quenched (ca. 10 K/min) in magnetic fields also splintered, while slowly cooled samples (ca. 0.8 K/min) did not show any signs of degradation over a period of days.

## Discussion

The reaction of $(MeCp)VCl_3$ and TmTTF results in three phases: $[TmTTF]_{1,2}[(MeCp)VCl_3]$ and the partial oxidation product $[TmTTF]_3[\{(MeCp)VCl_2\}_2O]_2$ (1). Compound 1 is a one-dimensional charge-transfer complex as determined by X-ray crystallography. The magnetic susceptibility of 1 is highly anisotropic and generally defines this complex as an $XY$ magnetic system, with ordering directions perpendicular to the $Z$ (or stacking $c$) axis, with an (zero temperature, zero field) antiferromagnetic ground state. At low fields and temperatures, the complex displays weak ferromagnetic coupling.[22] Complex 1 is not a (three-dimensional) ferromagnet, as the data indicate no spontaneous magnetization nor sharp transitions indicative of extensive long-range order. Even so, the susceptibility observed is greater than that attributable to spin-only components.

Since no theoretical model yet exists to describe this compound, the factors leading to cooperative magnetic behavior may be defined only in general terms. The primary susceptibility enhancement in the $b$ direction may result from a lack of orbital overlap between the stacks.[23] Additionally, the effect onset temperature of ca. 50 K appears much too low to include a sizable spin contribution from the $S = {}^3/_2$ state of a (+)D split vanadium dimer.[24] This increases the significance of an already greater than spin-only observed susceptibility. The $a$-axis ordering could be short-range ordering of the widely separated $V^{IV}$ ($d^1$) sites. Finally, spin pairing within the organic stack

(22) (a) Bellitto, C.; Filaci, P.; Patrizio, S. *Inorg. Chem.* **1987**, *26*, 191. (b) Bellitto, C.; Day, P.; Wood, T. E. *J. Chem. Soc., Dalton Trans.* **1978**, 1207.

(23) Pei, Y.; Journaux, Y.; Kahn, O. *Inorg. Chem.* **1989**, *28*, 100.

(24) A noticeable lack of magnetically characterized V–O–V dimers makes this difficult to confirm, however reasonable.

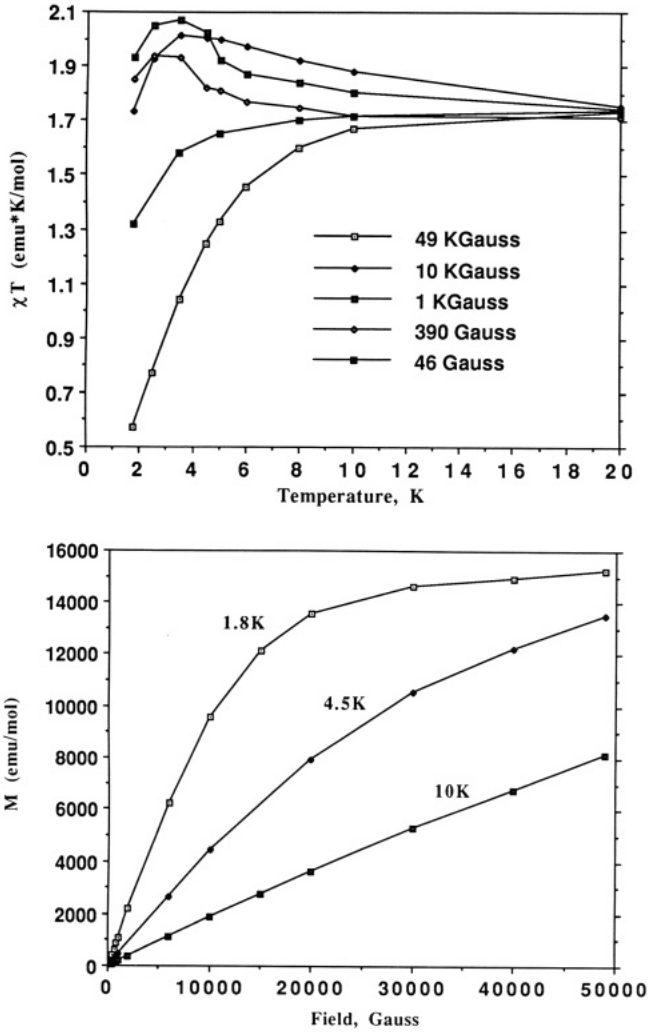


**Figure 7.** Polycrystalline $[TmTTF]_3[\{(MeCp)VCl_2\}_2O]_2$: $\chi T$ versus temperature (below 20 K) at various applied fields (top), and magnetization versus applied field at various temperatures (bottom).

(*c* axis) likely initiates the final antiferromagnetic coupling at 3.5 K (which may be associated with the weak Cl···S and hydrogen bonding interstack contacts).

The overall susceptibility at higher fields is indicative of a collapsing two-spin-state system. The magnetic transition is notably *not* classical metamagnetism:[25] the salt exhibits a low-field ferromagnetic to high-field antiferromagnetic transition. This highly atypical behavior can currently be noted only without suitable quantitative explanation.

The difference between single-crystal and polycrystalline susceptibility implies that the crystals may be displaying more long-range order than the crushed samples. The anomalous magnetic behavior of polycrystalline samples may be explained by a defect site model[26] or by the introduction of circuit states.[27] The defects inhibit long-range cooperative behavior and change the low-field ground state from apparent ferromagnetic to antiferromagnetic. In the present case a critical field ($0 < H_c < 1000$ G) is required to overcome the defect boundaries.

The observation of both crystal instability and the discontinuity in magnetic behavior at 50 K may indicate that a structural phase transition accompanies cooperative magnetic behavior. Thus the room-temperature structure may not adequately reflect the solid-state environment under 50 K. One possible structural change that satisfies the criterion that the cleavage plane be normal to the *c* axis as well as creating a more symmetric (and hence more likely cooperative) structure is movement within the TmTTF stack:

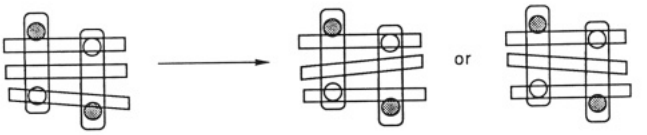


A movement from an A·A·B stacking pattern to an A·B·A pattern may be a relatively low energy since the difference in distances between average TmTTF planes is only 0.05 Å (at room temperature).

One aspect of the interpretation of strongly coupled vanadium dimers modulating the TmTTF stack is that such a model would resemble the virtual forward (or retro) charge-transfer doctrine (McConnell theory[28]) which has been used to describe the molecular ferromagnet $[(Me_5C_5)_2Fe][TCNE]$. In the present case, the two-electron three-orbital TmTTF stack serves as the non-half-filled molecular orbital giving rise to ferromagnetic coupling. On the other hand, recent successes in the ferromagnetic CuMn systems[29] have shown how effectively large magnetic centers ($\{(MeCp)VCl_2\}_2O^-$) may be modulated by small well-placed magnetic dipoles ($[TmTTF]_{1.5}^+$) to give ferromagnetic character.

## Conclusion

The novel organometallic acceptor charge-transfer salt $[TmTTF]_3[\{(MeCp)VCl_2\}_2O]_2$ displays weak ferromagnetic coupling between mixed-valence cations and anions. The magnetic interaction is highly anisotropic ($XY$) as evidenced from molecular packing considerations. Magnetic and physical data are interpreted to indicate that the susceptibility enhancement is associated with a structural phase transition in the cation stack. The title complex provides further evidence that the synthesis of molecular ferromagnets is a rich area, and the title compound has proven to be a highly successful proof-of-concept material for solid-state syntheses with organometallic acceptors.

**Acknowledgment.** This paper would not have been possible without the attentive consideration of Profs. David N. Hendrickson and especially Thomas B. Rauchfuss. Scott R. Wilson and Charlotte Stern are thanked for their preparation of crystallographic tables. D.B.M. gratefully notes the financial support of Roger Adams and 3M Corp. Fellowships. The research was supported by a grant from the Department of Energy (DE-AC02-76ER01198).

**Registry No.** 1, 124399-81-1; TmTTF, 50708-37-7; [TmTTF][(MeCp)$VCl_3$], 113378-54-4; $[TmTTF]_2$[(MeCp)$VCl_3$], 124399-82-2; (MeCp)$VCl_3$, 111005-01-7.

**Supplementary Material Available:** Tables of thermal parameters and magnetic susceptibility data (8 pages); final observed and calculated structure factors (17 pages). Ordering information is given on any current masthead page.

(25) Carlin, R. L. *Magnetochemistry*; Springer-Verlag: Berlin, 1986.
(26) O'Connor, C. J. *Progress in Inorganic Chemistry*; Lippard, S. J., Ed.; Wiley: New York, 1982; Vol. 29, p 238.
(27) Holczer, K.; Gruner, G.; Miljak, M.; Cooper, J. *Solid State Commun.* **1977**, *24*, 97.
(28) (a) McConnell, H. M. *J. Phys. Chem.* **1963**, *39*, 1910. (b) Miller, J. S.; Epstein, A. J. *J. Am. Chem. Soc.* **1987**, *109*, 3850.
(29) Lloret, F.; Nakatani, K.; Journaux, Y.; Kahn, O.; Pei, Y.; Renard, J. P. *J. Chem. Soc., Chem. Commun.* **1988**, 642.